# Second nearest-neighbor modified embedded atom method potentials for bcc transition metals

Byeong-Joo Lee,[1,*] M.I. Baskes,[2,†] Hanchul Kim,[1] and Yang Koo Cho[1]
[1]*Materials Evaluation Center, Korea Research Institute of Standards and Science, Yusong P.O. Box 102, Taejon 305-600, Republic of Korea*
[2]*Structure/Properties Relation Group, Los Alamos National Laboratory, MS G755, Los Alamos, New Mexico 87545*
(Received 10 May 2001; published 15 October 2001)

The second nearest-neighbor modified embedded atom method (MEAM) [Phys. Rev. B 62, 8564 (2000)], developed in order to solve problems of the original first nearest-neighbor MEAM on bcc metals, has now been applied to all bcc transition metals, Fe, Cr, Mo, W, V, Nb, and Ta. The potential parameters could be determined empirically by fitting to $(\partial B/\partial P)$, elastic constants, structural energy differences among bcc, fcc and hcp structures, vacancy-formation energy, and surface energy. Various physical properties of individual elements, including elastic constants, structural properties, point-defect properties, surface properties, and thermal properties were calculated and compared with experiments or high level calculations so that the reliability of the present empirical atomic-potential formalism can be evaluated. It is shown that the present potentials reasonably reproduce nonfitted properties of the bcc transition metals, as well as the fitted properties. The effect of the size of radial cutoff distance on the calculation and the compatibility with the original first nearest-neighbor MEAM that has been successful for fcc, hcp, and other structures are also discussed.

DOI: 10.1103/PhysRevB.64.184102 PACS number(s): 61.50.Lt, 62.20.Dc, 64.70.Dv, 64.70.Kb

## I. INTRODUCTION

Semiempirical atomic potentials enable large-scale atomistic simulation (molecular dynamics or Monte Carlo simulation) useful in the study of solid-state phase transformations. In order to apply the technique to alloys, it is convenient to describe the atomic potentials of various elements with various crystal structures using a common formalism. The modified embedded atom method (MEAM) potential proposed by Baskes and coworkers[1–4] may be said to be unique among empirical potentials in that it can reproduce physical properties of many elements with various crystal structures including hcp and diamond cubic as well as fcc and bcc using the same formalism.

However, when being applied to an atomistic simulation on some bcc metals, the MEAM reveals some critical shortcomings. First, for many bcc metals, the surface energy of the (111) surface is computed to be smaller than that of the (100) surface, which is contrary to experimental results.[5,6] Second, more seriously, a structure more stable than the original bcc is created during a molecular dynamics simulation of some bcc metals (Fe, Cr, Mo, etc.). This newly created structure has quite different elastic properties compared to the metals with the original structure. Simply changing the model parameters cannot solve these problems without compromising the descriptions for other physical properties.

The MEAM was formulated to consider only nearest-neighbor interactions by using a strong screening function.[3,7,8] However, in the bcc structure, the second nearest-neighbor distance is larger than the first nearest-neighbor distance by only about 15%. The interactions between second nearest-neighbor atoms in bcc may not be negligible even with the screening. It could be thought that the failure of the MEAM in reproducing the surface energies of low-index surfaces in correct order originates from the fact that only the nearest-neighbor interactions are considered in the model.

Recently, the present authors solved the above-mentioned problems of the MEAM for bcc metals by modifying the original MEAM formalism to partially consider the second nearest-neighbor interactions as well as the first nearest-neighbor interactions.[9] The second nearest-neighbor interactions could be taken into consideration by adjusting the screening. A potential in this formalism successfully reproduced many physical properties of Fe.

The purpose of the present work is to apply the second nearest-neighbor MEAM to a large number of bcc elements and to show that the improvements obtained for Fe[9] can be transferred to other bcc metals (Cr, Mo, W, V, Nb, Ta). In Sec. II, the formalism of the second nearest-neighbor MEAM (2NN MEAM) will be described paying attention to the difference from the original first nearest-neighbor MEAM (1NN MEAM).[3] In Sec. III, the procedure for determination of parameter values will be given. Comparisons between some calculated and experimental physical properties of the bcc metals will be given in Sec. IV. Applicability and limit of the present 2NN MEAM will also be discussed in this section, and Sec. V is a summary.

## II. FORMALISM

### A. First and second nearest-neighbor MEAM for elements

In the original 1NN MEAM,[1–4] the total energy of a system is approximated as

$$E=\sum_i \left[ F(\overline{\rho}_i)+\frac{1}{2}\sum_{j(\neq i)} \phi(R_{ij}) \right], \tag{1}$$

where $F$ is the embedding function, $\overline{\rho}_i$ is the background electron density at site $i$, and $\phi(R_{ij})$ is the pair interaction between atoms $i$ and $j$ separated by a distance $R_{ij}$. Concerning Eq. (1), what is actually done in atomistic simulations is the calculation of energy using the expression on the right-

 

hand side of Eq. (1), based on given positions of individual atoms. For this, the functional forms for the two terms, $F$ and $\phi$ should be given.

The embedding function is given as follows:

$$F(\overline{\rho}) = AE_c(\overline{\rho}/\overline{\rho}^0)\ln(\overline{\rho}/\overline{\rho}^0). \tag{2}$$

Here, $A$ is an adjustable parameter, $E_c$ is the sublimation energy, and $\overline{\rho}^0$ is the background electron density for a reference structure. The reference structure is a structure where individual atoms are on the exact lattice points without deviation. Normally, the equilibrium structure is taken as the reference structure for elements. The background electron density $\overline{\rho}_i$ is composed of a spherically symmetric partial electron density $\rho_i^{(0)}$ and the angular contributions $\rho_i^{(1)}$, $\rho_i^{(2)}$, and $\rho_i^{(3)}$. Each partial electron density term has the following form,

$$(\rho_i^{(0)})^2 = \left[\sum_{j\neq i} \rho_j^{a(0)}(R_{ij})\right]^2, \tag{3a}$$

$$(\rho_i^{(1)})^2 = \sum_{\alpha} \left[\sum_{j\neq i} \frac{R_{ij}^{\alpha}}{R_{ij}} \rho_j^{a(1)}(R_{ij})\right]^2, \tag{3b}$$

$$(\rho_i^{(2)})^2 = \sum_{\alpha,\beta} \left[\sum_{j\neq i} \frac{R_{ij}^{\alpha}R_{ij}^{\beta}}{R_{ij}^2} \rho_j^{a(2)}(R_{ij})\right]^2 - \frac{1}{3}\left[\sum_{j\neq i} \rho_j^{a(2)}(R_{ij})\right]^2, \tag{3c}$$

$$(\rho_i^{(3)})^2 = \sum_{\alpha,\beta,\gamma} \left[\sum_{j\neq i} \frac{R_{ij}^{\alpha}R_{ij}^{\beta}R_{ij}^{\gamma}}{R_{ij}^3} \rho_j^{a(3)}(R_{ij})\right]^2 - \frac{3}{5}\sum_{\alpha} \left[\sum_{j\neq i} \frac{R_{ij}^{\alpha}}{R_{ij}} \rho_j^{a(3)}(R_{ij})\right]^2. \tag{3d}$$

Here, $\rho_j^{a(h)}$ represent atomic electron densities from $j$ atom at a distance $R_{ij}$ from atom $i$. $R_{ij}^{\alpha}$ is the $\alpha$ component of the distance vector between atoms $j$ and $i$ ($\alpha = x,y,z$). The expression for $(\rho_i^{(3)})^2$ [Eq. (3d)] is a recent modification to make the partial electron densities orthogonal.[10] The way of combining the partial electron densities to give the total background electron density is not unique, and several expressions have been proposed.[8] Among them, the following form is used in the present work.

$$\overline{\rho}_i = \rho_i^{(0)} G(\Gamma_i) \tag{4}$$

where

$$G(\Gamma) = 2/(1+e^{-\Gamma}) \tag{5}$$

and

$$\Gamma_i = \sum_{h=1}^{3} t^{(h)}[\rho_i^{(h)}/\rho_i^{(0)}]^2, \tag{6}$$

$t^{(h)}$ are adjustable parameters. The atomic electron density is given as

$$\rho^{a(h)}(R) = \exp[-\beta^{(h)}(R/r_e - 1)], \tag{7}$$

where $\beta^{(h)}$ are adjustable parameters and $r_e$ is the nearest-neighbor distance in the equilibrium reference structure.

Now, the embedding function can be computed. What should be done next for the energy calculation is to compute the pair interaction terms. For this, the functional form of the pair interaction $\phi(R)$ is necessary. However, in the MEAM, no specific functional expression is given directly to $\phi(R)$. Instead, the energy per atom for the equilibrium reference structure is given a value as a function of atomic volume (nearest-neighbor distance). Then, the value of $\phi(R)$ is computed from the known values of the total energy and the embedding function, as a function of nearest-neighbor distance $R$.

The value of the energy per atom for the equilibrium reference structure is obtained from the zero-temperature universal equation of state by Rose *et al.*[11] as a function of nearest-neighbor distance $R$.

$$E^u(R) = -E_c(1 + a^* + da^{*3})e^{-a^*} \tag{8}$$

where $d$ is an adjustable parameter, and

$$a^* = \alpha(R/r_e - 1) \tag{9}$$

and

$$\alpha = (9B\Omega/E_c)^{1/2}. \tag{10}$$

Here $E^u(R)$ is the universal function for a uniform expansion or contraction in the reference structure, $B$ is the bulk modulus, and $\Omega$ is the equilibrium atomic volume.

In the 1NN MEAM, only the first nearest-neighbor interactions are considered as already mentioned. The summation of pair interaction terms in Eq. (1) is performed over only nearest-neighbor atoms. Here, it should be noted that the bonding directions among neighbor atoms are fixed in a reference structure and the embedding function becomes a function of only nearest-neighbor distance $R$. Therefore, for a reference structure, the energy per atom can be written again as follows, as a function of only the nearest-neighbor distance $R$.

$$E^u(R) = F[\overline{\rho}^0(R)] + (Z_1/2)\phi(R), \tag{11}$$

where $Z_1$ is the number of nearest-neighbor atoms. The expressions for the embedding function $F$ and energy per atom $E^u(R)$ are now available [from Eqs. (2) and (8), respectively]. The expression for the pair interaction between two atoms separated by a distance R, $\phi(R)$, is obtained from Eq. (11) as follows,

$$\phi(R) = (2/Z_1)\{E^u(R) - F[\overline{\rho}^0(R)]\}. \tag{12}$$

The key difference of the 2NN MEAM from the 1NN MEAM is that second nearest-neighbor interactions are partially considered during the procedure of determining $\phi(R)$ values. In the 1NN MEAM, the neglect of the second nearest-neighbor interactions is made by the use of a strong many-body screening function. In the same way, the consideration of the second nearest-neighbor interactions in the 2NN MEAM is also made by adjusting the many-body screening function so that it becomes less severe.

The amount of screening of a $k$ atom to the interaction between $i$ and $j$ atoms is determined using a simple geometric construction.[7,8] Imagine an ellipse on an $(x,y)$ plane, passing through atoms $i$, $k$, and $j$ with the $x$ axis of the ellipse determined by atoms $i$ and $j$. The equation of the ellipse is given by

$$x^2+(1/C)y^2=\left(\frac{1}{2}R_{ij}\right)^2. \tag{13}$$

For each $k$ atom, the $C$ value can be computed from the relative distances among the three atoms $i$, $j$, and $k$. Each $C$ value defines an ellipse with its own $y$-axis length. The basic idea for the amount of screening is as follows. Two values, $C_{max}$ and $C_{min}$ ($C_{max}>C_{min}$) are given, so that two ellipses with different length of $y$ axis can be defined. If a $k$ atom is located outside of the larger ellipse defined by $C_{max}$, that is, if $C$ value for a $k$ atom is larger than $C_{max}$, it is assumed that the $k$ atom does not give any effect on the $i$-$j$ interaction. In this case, the screening factor is 1. If $C$ value for a $k$ atom is smaller than $C_{min}$, then it is assumed that the $k$ atom completely screen the $i$-$j$ interaction. In this case, the screening factor becomes zero. Between the two $C$ values ($C_{max}$ and $C_{min}$), the screening factor changes gradually. The resultant many-body screening function between atoms $i$ and $j$ is defined as the product of the screening factors due to all other neighbor atoms $k$. The screening function is then multiplied to the atomic electron densities and pair potential.

In the original 1NN MEAM,[3] $C_{max}=2.8$ and $C_{min}=2.0$ were chosen so that the first nearest-neighbors are completely unscreened for reasonably large thermal vibration in the fcc structure and the interactions are still the first neighbor only even in the bcc structure. In the present 2NN MEAM, the second nearest-neighbor interactions are taken into consideration by giving a lower value than 2.0 (1.0) to $C_{min}$ for bcc (fcc) structure. Consideration of second nearest-neighbor interactions does not change the formalism in Eqs. (1)–(10). However, for computation of pair interactions the summation should be extended to the second nearest-neighbor atoms. Taking the second nearest-neighbor interactions into consideration, the energy per atom for a reference structure is now expressed as follows:

$$E^u(R)=F[\overline{\rho}^0(R)]+(Z_1/2)\phi(R)+(Z_2S/2)\phi(aR). \tag{14}$$

Here, $Z_2$ is the number of second nearest-neighbor atoms, and $a$ is the ratio between the second and first nearest-neighbor distances. $S$ is the screening function on the second nearest-neighbor interactions. It should be noted that the screening function $S$ is a constant for a given reference structure, if a value is given to $C_{max}$ and $C_{min}$. By introducing another pair potential, $\psi(R)$, Eq. (14) can be written again as follows:

$$E^u(R)=F[\overline{\rho}^0(R)]+(Z_1/2)\psi(R) \tag{15}$$

where

$$\psi(R)=\phi(R)+(Z_2S/Z_1)\phi(aR). \tag{16}$$

Now, $\psi(R)$ can be calculated from Eq. (15) as a function of $R$. Then, the pair potential $\phi(R)$ is calculated using the following relation, also as a function of $R$,

$$\phi(R)=\psi(R)+\sum_{n=1}(-1)^n(Z_2S/Z_1)^n\psi(a^nR). \tag{17}$$

Here, the summation is performed until the correct value of energy is obtained for the equilibrium reference structure.

It should be noted here that at low values of $C_{min}$ ($<0.47$ for bcc), even third nearest-neighbor interactions are not completely screened. If such interactions are included in the calculation, it will cause an inconsistency and an error in energy calculations, because only the interactions between first and second nearest-neighbors are considered when defining the pair interaction in Eqs. (14)–(17). The size of such an error is small because the interaction between third nearest-neighbor atoms is small due to the many-body screening. For example, for Fe ($C_{min}=0.36$) and Ta ($C_{min}=0.25$), the errors in the calculated equilibrium potential energies are 0.004% and 0.02%, respectively. In the present study, this inconsistency is accepted because the error is negligibly small. The effect of such third nearest-neighbor interactions are minimized by using a radial cutoff function with a cutoff distance between second and third nearest-neighbor distances.

### B. Application to alloy systems

The above is a brief review of the 1NN and 2NN MEAM formalism for elements. The application of the MEAM is not confined to descriptions of elements, but can be extended to descriptions of alloy systems. A method to describe binary alloy systems has been presented for the 1NN MEAM.[3] Owing to the importance of describing alloy systems, it will be shown here that the same method can be applied for alloy description using the 2NN MEAM, even though alloy systems are not covered in the present paper.

To describe an alloy system, the pair interaction between different elements should be determined. For this, a similar technique that was used to determine pair interaction for elements, Eq. (11) or Eq. (14), is applied to binary alloy systems. In the 1NN MEAM,[3] a perfectly ordered binary intermetallic compound, where only one type of atom has different type of atoms as first nearest-neighbors, is considered as a reference structure. The $B1$ (NaCl type) or $B2$ (CsCl type) ordered structures can be good examples. For such a reference structure, the total energy per atoms (for $\frac{1}{2}i$ atom + $\frac{1}{2}j$ atom), $E_{ij}^u(R)$, is given by

$$E_{ij}^u(R)=\frac{1}{2}[F_i(\overline{\rho}_i)+F_j(\overline{\rho}_j)+Z^{ij}\phi_{ij}(R)], \tag{18}$$

where $Z^{ij}$ is the number of nearest-neighbors in the reference structure. Equation (18) can be written for $\phi_{ij}(R)$ as

$$\phi_{ij}(R)=\frac{1}{Z^{ij}}[2E_{ij}^u(R)-F_i(\overline{\rho}_i)-F_j(\overline{\rho}_j)]. \tag{19}$$

TABLE I. Parameters for the second nearest-neighbor MEAM (2NN MEAM) potential of Fe, Cr, Mo, W, V, Nb and Ta. The units of the sublimation energy $E_c$, the equilibrium nearest-neighbor distance $r_e$ and the bulk modulus $B$ are eV, Å, and $10^{12}$dyn/cm$^2$, respectively.

| | $E_c$ | $r_e$ | $B$ | $A$ | $\beta^{(0)}$ | $\beta^{(1)}$ | $\beta^{(2)}$ | $\beta^{(3)}$ | $t^{(1)}$ | $t^{(2)}$ | $t^{(3)}$ | $C_{max}$ | $C_{min}$ | $S$ | $d$ |
|---|---|---|---|---|---|---|---|---|---|---|---|---|---|---|---|
| Fe | 4.29 | 2.480 | 1.73 | 0.56 | 4.15 | 1.0 | 1.0 | 1.0 | 2.6 | 1.8 | −7.2 | 2.80 | 0.36 | 0.9112 | 0.05 |
| Cr | 4.10 | 2.495 | 1.90 | 0.42 | 6.81 | 1.0 | 1.0 | 1.0 | 0.3 | 5.9 | −10.4 | 2.80 | 0.78 | 0.8193 | 0.00 |
| Mo | 6.81 | 2.725 | 2.65 | 0.46 | 7.03 | 1.0 | 1.0 | 1.0 | 0.5 | 3.1 | −7.5 | 2.80 | 0.64 | 0.8590 | 0.00 |
| W | 8.66 | 2.740 | 3.14 | 0.40 | 6.54 | 1.0 | 1.0 | 1.0 | −0.6 | 0.3 | −8.7 | 2.80 | 0.49 | 0.8905 | 0.00 |
| V | 5.30 | 2.625 | 1.57 | 0.73 | 4.74 | 1.0 | 2.5 | 1.0 | 3.3 | 3.2 | −2.0 | 2.80 | 0.49 | 0.8905 | 0.00 |
| Nb | 7.47 | 2.860 | 1.73 | 0.72 | 5.08 | 1.0 | 2.5 | 1.0 | 1.7 | 2.8 | −1.6 | 2.80 | 0.36 | 0.9112 | 0.00 |
| Ta | 8.09 | 2.860 | 1.94 | 0.67 | 4.49 | 1.0 | 1.0 | 1.0 | 1.7 | 2.1 | −3.2 | 2.80 | 0.25 | 0.9251 | 0.00 |

The embedding functions $F_i$ and $F_j$ can always be computed. To obtain the value of $E_{ij}^u(R)$, the universal equation of state[11] is considered once again for the reference phase (intermetallic compound). Assumed values or experimentally measured values of $E_c$, $r_e$ (or $\Omega$) and $B$ for the reference phase is given. Then the pair interaction between $i$ and $j$ atoms is determined as a function of interatomic distance.

The above method can be equally applied in the 2NN MEAM. In the 1NN MEAM, the reference binary alloy structure was a structure where the first nearest-neighbors of an atom are all different type. The additional condition that is given to the reference structure in the 2NN MEAM is that the second nearest-neighbors should all be of the same type. This condition is satisfied in both of the $B1$ and $B2$ ordered structures. Considering the second nearest-neighbor interactions, Eq. (18) is now rewritten as

$$E_{ij}^u(R)=\frac{1}{2}\left\{F_i(\overline{\rho_i})+F_j(\overline{\rho_j})+Z^{ij}\phi_{ij}(R)+\frac{1}{2}Z_2^{ij}(\phi_{ii}(aR)+\phi_{jj}(aR))\right\}, \tag{20}$$

$Z_2^{ij}$ is the number of second nearest-neighbor atoms in the reference structure. $\phi_{ii}$ and $\phi_{jj}$ are pair interactions between $i$ atoms and between $j$ atoms, respectively. $a$ is the ratio between the second and first nearest-neighbor distances. The procedure of computing $\overline{\rho_i}$ and $\overline{\rho_j}$ is not different from that in 1NN MEAM except that the contribution from the second nearest-neighbors should also be considered. The pair interactions between the same type of atoms can be computed from the descriptions of individual elements. The value of $E_{ij}^u(R)$ is obtained using the same procedure as in the 1NN MEAM. Therefore, the pair interaction between the different types of atoms can be computed using the following expression, as a function of interatomic distance.

$$\phi_{ij}(R)=\frac{1}{Z_{ij}}\left\{2E_{ij}^u(R)-F_i(\overline{\rho_i})-F_j(\overline{\rho_j})-\frac{1}{2}Z_2^{ij}[\phi_{ii}(aR)+\phi_{jj}(aR)]\right\}. \tag{21}$$

Though more computing effort is necessary, the 2NN MEAM does not cause any additional difficulty in the descriptions of alloy systems, compared to the 1NN MEAM.

## III. DETERMINATION OF THE PARAMETERS

The formalism (2NN MEAM) for elements was applied to evaluate the MEAM parameters for the bcc transition metals, Fe, Cr, Mo, W, V, Nb, and Ta. The parameters were determined by fitting to physical properties of each element, as will be described. The parameters finally determined for individual elements are listed in Table I. Here, the reference structure is bcc for all elements. In this section, the procedure for the determination of these parameter values is presented.

The 2NN MEAM formalism gives 15 model parameters as shown in Table I. Here, the amount of screening between second nearest-neighbor atoms $S$ is not an independent parameter, but is uniquely determined if the $C_{max}$, $C_{min}$ values, and the reference structure are given. The values of the sublimation energy $E_c$, nearest-neighbor distance $r_e$, and the bulk modulus $B$ are given experimentally. Therefore, the actual number of adjustable parameters is 11.

Of the 11 adjustable parameters (those listed in Table I except $E_c$, $r_e$, $B$, and $S$), $C_{max}$ was given the same value (2.8) as in the 1NN MEAM.[3] For $\beta^{(1)}$, $\beta^{(2)}$ and $\beta^{(3)}$, it was also intended to keep the same values (all 1.0) as in the 1NN MEAM (Ref. 3) because the effect of those parameters on the physical properties considered here was meager. (However, some different values had to be given to $\beta^{(2)}$ for some elements [Nb and V] as will be mentioned later on.) By fixing the values of $\beta^{(1)}$, $\beta^{(2)}$, and $\beta^{(3)}$, the adjustable parameters whose values should be actually determined by fitting to physical properties becomes only seven, $A$, $\beta^{(0)}$, $t^{(1)}$, $t^{(2)}$, $t^{(3)}$, $C_{min}$, and $d$.

As already mentioned, the solid-state phase transformation is a good research field where the atomistic simulation using semiempirical potentials can be a powerful technique. Especially, the initial stage of phase transformation (nucleation stage) cannot be quantitatively described by any other analytic approaches. The three important terms in nucleation kinetics are the driving force, interfacial energy, and the misfit strain energy. Therefore, in order to be practically applicable, it is believed that the semiempirical atomic potentials should be able to reproduce at least the above three kinds of properties of elements correctly. In the present study, the adjustable parameters are determined numerically so that the structural energy differences (energy differences between bcc and fcc, and fcc and hcp structures), defect energies (surface energy and vacancy formation energy), and elastic properties

TABLE II. $(\partial B/\partial P)$ at 0 K by the first-principles calculation, at RT from experiments and 2NN MEAM value (0 K) obtained using $d=0$ and $d=0.05$ for individual elements. The FP calculation values are those obtained in the present study using the VASP (Ref. 14) and the experimental data are from Ref. 11.

| | FP (0 K) | Experimental data (RT) | 2NN MEAM $d=0$ | 2NN MEAM $d=0.05$ |
|---|---|---|---|---|
| Fe | 4.63 | 5.29 | 4.44 | 4.95 |
| Cr | 4.08 | | 4.72 | 5.28 |
| Mo | 4.25 | 4.7 | 4.89 | 5.48 |
| W | 4.20 | 4.5 | 4.79 | 5.36 |
| V | 3.68 | | 4.21 | 4.69 |
| Nb | 3.64 | 4.1 | 4.23 | 4.71 |
| Ta | | 3.8 | 4.28 | 4.78 |

(elastic constants) are reproduced.

It should be noted here that the $da^{*3}$ term was newly introduced into the present formalism for the energy per atom of the reference structure [Eq. (8)], compared to the 1NN MEAM. Actually, this term had been included in the original universal equation of state[11] with a value of 0.05 for $d$, which was fixed from the thermal expansion of Cu. However, generally, almost the same degree of agreement, and for some elements, even better agreement between calculated and experimental pressure-volume relation could be obtained without this term. This term has always been ignored in the 1NN MEAM formalism[1–4] and even in the initial formulation of the 2NN MEAM.[9] However, during the present study, it was found that the ignorance of the $da^{*3}$ term can cause somewhat large disagreement with the experimental pressure-volume relation for some elements. It was finally decided to take $d$ as a material-dependent parameter.

The value of $d$ could be determined separately from other adjustable parameters, using the $(\partial B/\partial P)$ value from either first-principles (FP) calculation or from experiments. Because experimental data for $(\partial B/\partial P)$ were not always available, first-principles calculation could yield this information for the determination of $d$. The present authors have performed the *ab initio* pseudopotential calculations within the generalized gradient approximation (GGA)[12,13] using the Vienna *ab initio* simulation package (VASP).[14] The atoms are represented by ultrasoft Vanderbilt-type pseudopotentials as supplied by Kresse and Hafner.[15] The FP calculated and experimental $(\partial B/\partial P)$ values for each element are compared with the 2NN MEAM values calculated for $d=0$ and $d=0.05$, in Table II.

The FP calculation reproduces the trend of experimental $(\partial B/\partial P)$ values among the elements correctly, even though the absolute agreement with experimental data is not very good. Of course, a very good agreement could not be expected because the FP values were for 0 K while the experimental data were usually for room temperature (RT). However, the differences were much larger than those between 0 K and RT values calculated in the present study using the 2NN MEAM. (These were smaller than 0.1 for Fe and Mo). The large differences between the FP calculation and experiments made it impossible to evaluate the $d$ value as a material-dependent parameter. However, it was possible to judge which of the two 2NN MEAM values, one based on $d=0$ or the other based on $d=0.05$, would be closer to the real $(\partial B/\partial P)_{T=0}$ value. Therefore, it was finally decided to select the value of $d$ for each element between 0 and 0.05, according to FP calculation or experimental $(\partial B/\partial P)$ value if available. By this, the selected $d$ value of Fe was 0.05 while it was zero for other bcc metals considered. Figure 1 shows the normalized energy $(E/E_C)$ vs normalized volume $(V/V_o)$ for Fe. The curve is by the present 2NN MEAM and the symbols are first-principles calculations also by the present authors using the VASP.[14]

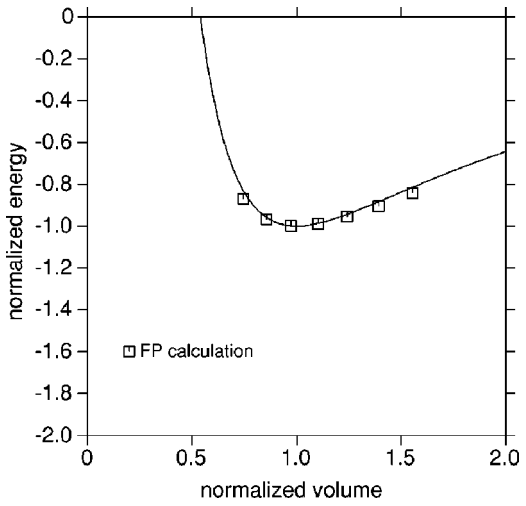


FIG. 1. Calculated normalized energy $(E/E_c)$ vs normalized volume $(V/V_o)$ for Fe, by the present 2NN MEAM. Symbols are first-principles calculations.

The determination of $d$ value is done at the beginning of the parametrization procedure. Then, the $A$, $\beta^{(0)}$, $t^{(1)}$, $t^{(2)}$, $t^{(3)}$, and $C_{min}$ values are determined looking at the structural energy differences $(\Delta E_{bcc\rightarrow fcc}, \Delta E_{fcc\rightarrow hcp})$, surface energy $E_{(surf)}$, vacancy formation energy $E_v^f$ and elastic constants $(C_{11}, C_{12}, C_{44})$, as already mentioned. Generally, the effect of each parameter on individual properties is complicated, and it is impossible to relate one property to one parameter. However, the effects of some parameters are certainly confined to only few properties, and the evaluation of parameters can be done systematically. Table III shows the relationship between parameters and properties discovered

TABLE III. Effect of parameters on individual properties for bcc elements. The plus sign means the effect is significant, the minus sign means the effect is minor, and no sign means no effect.

| | $A$ | $\beta^{(0)}$ | $t^{(1)}$ | $t^{(2)}$ | $t^{(3)}$ | $C_{min}$ |
|---|---|---|---|---|---|---|
| $C_{11}$ and $C_{12}$ | + | + | | − | | + |
| $C_{44}$ | + | + | | − | | + |
| $E_{(surf)}$ | + | − | + | − | − | − |
| $E_v^f$ | + | − | + | + | + | + |
| $\Delta E_{bcc\rightarrow fcc}$ | + | + | | | | + |
| $\Delta E_{fcc\rightarrow hcp}$ | + | + | | | + | + |

during the fitting procedure for bcc elements. Here, the plus sign means the effect is significant, the minus sign means the effect is minor, and no sign means no effect.

$C_{11}$ and $C_{12}$ are not independent from each other for a given bulk modulus. First, an arbitrary value is given to $C_{min}$. Then, the values of $A$ and $\beta^{(0)}$ are determined fitting $C_{11}$ and $C_{44}$ exactly. This procedure does not necessarily give a correct value for the bcc/fcc energy difference $\Delta E_{bcc\rightarrow fcc}$. Changing the $C_{min}$ value, this procedure is repeated until satisfactory values are obtained for $\Delta E_{bcc\rightarrow fcc}$ as well as the elastic constants. Now, $t^{(3)}$ can be determined exclusively looking at $\Delta E_{fcc\rightarrow hcp}$. Then, $t^{(1)}$ and $t^{(2)}$ are determined fitting the surface energies and vacancy-formation energy. The last step can cause a change in the elastic constants of the model element because of the new value of $t^{(2)}$. This change can be removed by slightly changing the $A$ and $\beta^{(0)}$ values and repeating the procedure. Finally, a molecular-dynamics run is performed in order to check whether the parameter set stabilizes the bcc structure until melting.

Using the relationships in Table III, it was usually possible to exactly reproduce the target value of a property. However, it was generally impossible to reproduce the target values of all properties, simultaneously. Among all properties considered, it was believed that the elastic constants are those most accurately measured. Therefore, the determination of parameters was done so that the elastic constants are exactly reproduced, and so that the other property values are reasonably reproduced considering their accuracy. In the 1NN MEAM, the fitting to the elastic constants has been performed using room-temperature data, giving RT value of bulk modulus to $B$.[3,4] However, in the present work, a value at 0 K or at a low temperature close to 0 K was used for $B$ in order to calculate $(\partial B/\partial P)$ more accurately and determine $d$ value more correctly. Therefore, the fitting to the elastic constants was also performed using 0 K or low-temperature data. Concerning the surface energy, it was impossible to change the order among individual surface energies [for (100), (110), (111) surfaces] by adjusting the parameters, without severely losing good agreements for other properties. It was only intended to make the calculated lowest surface energy $[E_{(110)}]$ close to the average experimental value for polycrystals.

## IV. CALCULATION OF PHYSICAL PROPERTIES

The potentials determined by the above procedure were used to compute various physical properties of individual elements in order to evaluate the reliability of the 2NN MEAM. As well as the properties that have been used for fitting, the energy and equilibrium volume of simple cubic and diamond cubic structures, the activation energy of vacancy diffusion, the energy and structure of self-interstitial atoms, the relaxation of the (100), (110) and (111) surfaces, and thermal properties (thermal expansion coefficients, specific heat, melting point, heat of melting) were calculated and were compared with experimental data or high-level calculations. In this section, some comparisons between the present calculation and experimental data or high-level calculation will be presented. The reason why different value of $\beta^{(2)}$ has to be given to Nb and V will also be presented here. Then effect of radial cutoff distance on the calculated property values will be discussed.

TABLE IV. Calculated and experimental elastic constants ($10^{12}$ dyn/cm$^2$). Experimental data are from Ref. 16 except for Mo which are from Ref. 17.

| | $C_{11}$ | | $C_{12}$ | | $C_{44}$ | |
|---|---|---|---|---|---|---|
| | MEAM | expt. | MEAM | expt. | MEAM | expt. |
| Fe | 2.430 | 2.431 | 1.380 | 1.381 | 1.219 | 1.219 |
| Cr | 3.909 | 3.910 | 0.897 | 0.896 | 1.034 | 1.032 |
| Mo | 4.649 | 4.647 | 1.655 | 1.615 | 1.088 | 1.089 |
| W | 5.326 | 5.326 | 2.050 | 2.050 | 1.631 | 1.631 |
| V | 2.323 | 2.324 | 1.194 | 1.194 | 0.460 | 0.460 |
| Nb | 2.527 | 2.527 | 1.331 | 1.332 | 0.319 | 0.310 |
| Ta | 2.664 | 2.663 | 1.581 | 1.582 | 0.875 | 0.874 |

Table IV shows the calculated and experimental elastic constants ($C_{11}$, $C_{12}$, and $C_{44}$) for individual elements. The elastic constants were given the highest weight during fitting and could be reproduced almost exactly.

The calculated structural energy difference and volume of various crystal structures are listed in Table V. Among the items, only $\Delta E_{bcc\rightarrow fcc}$ and $\Delta E_{fcc\rightarrow hcp}$ are those used for fitting, and others are predicted. The experimental data being compared to the computed $\Delta E_{bcc\rightarrow fcc}$ and $\Delta E_{fcc\rightarrow hcp}$ are thermodynamically assessed values using the calphad method.[18] Here, the calculation on the hcp structure was done for a fixed ideal value of $c/a$, 1.633. For Fe, Cr, Mo, and W, the exact target values could be given to $\Delta E_{fcc\rightarrow hcp}$, while for V, Nb, and Ta, they were sacrificed in order to better fit to both of the vacancy formation energy and surface energy. The experimental information for the simple cubic and diamond structures is not available. A density-functional calculation[19] predicts that the energy of simple cubic and diamond structures of $3d$ metals are on the order of eV's above the bcc structure, which is in good agreement with the present prediction. The high-level calculation[19] gives the ratios of the simple cubic to bcc, and diamond to bcc atomic volume as about 1.1 and 1.4, respectively. For most elements, these ratios could be reproduced by the present 2NN MEAM. However, for V and Nb, the atomic volumes of simple cubic and diamond structures are somewhat too small.

The next property looked at was point defects. Besides the vacancy-formation energy, which was used for fitting, the activation energy of vacancy diffusion [(vacancy formation energy) + (vacancy migration energy)] could be calculated. As another type of point defect, the formation energy of a self-interstitial and its structure were also calculated. Table VI shows the calculated point-defect properties in comparison with experimental data for the vacancy-formation energy and activation energy of diffusion. Here, the calculated activation energy of vacancy diffusion is being compared with experimental data on the activation energy of diffusion assuming the vacancy mechanism of diffusion for transition metals. Generally, the vacancy formation energies could be

TABLE V. Calculated structural energy differences, $\Delta E$ (eV) and atomic volumes, $v/n$ (Å$^3$). The energies are relative to bcc except for hcp, where the energy is relative to fcc. The atomic volume of bcc, experimental data for the bcc→fcc and fcc→hcp energy differences are also presented for comparison.

| | bcc | fcc | | | hcp | | | Simple cubic | | Diamond | |
|---|---|---|---|---|---|---|---|---|---|---|---|
| | $v/n$ | $\Delta E_{bcc\to fcc}$ | expt. | $v/n$ | $\Delta E_{fcc\to hcp}$ | expt. | $v/n$ | $\Delta E_{bcc\to sc}$ | $v/n$ | $\Delta E_{bcc\to dia}$ | $v/n$ |
| Fe | 11.74 | 0.069 | 0.082[a] | 11.78 | −0.023[b] | −0.023[a] | 11.77 | 0.99 | 13.74 | 1.82 | 17.53 |
| Cr | 11.96 | 0.070 | 0.075[a] | 12.24 | −0.029[b] | −0.029[a] | 12.22 | 1.32 | 13.79 | 1.50 | 16.14 |
| Mo | 15.58 | 0.167 | 0.158[a] | 15.91 | −0.038[b] | −0.038[a] | 15.89 | 1.97 | 17.63 | 2.37 | 21.43 |
| W | 15.84 | 0.263 | 0.200[a] | 16.16 | −0.047[b] | −0.047[a] | 16.14 | 2.61 | 18.15 | 3.70 | 22.65 |
| V | 13.92 | 0.084 | 0.078[a] | 14.02 | −0.011[b] | −0.036[a] | 14.01 | 0.78 | 14.06 | 1.22 | 16.65 |
| Nb | 18.01 | 0.176 | 0.140[a] | 18.11 | −0.012[b] | −0.036[a] | 18.10 | 0.90 | 17.70 | 1.44 | 19.96 |
| Ta | 18.01 | 0.148 | 0.166[a] | 18.14 | −0.023[b] | −0.041[a] | 18.12 | 1.32 | 19.21 | 2.51 | 24.10 |

[a]Thermodynamically assessed values (room temperature data).[18]
[b]Calculated for the ideal value of c/a, 1.633.

reproduced in good agreement with experiments, while the vacancy-migration energies and thus the activation energies of diffusion were somewhat smaller than experimental data. Concerning the self-interstitials, it is experimentally known that the self-interstitials form dumbbell pairs along the [110] direction in the case of Fe and Mo.[20] According to the present 2NN MEAM, the self-interstials form a dumbbell pair along the same [110] direction for all bcc elements considered.

The surface properties (surface energy, energy anisotropy, and relaxation) are a good test bed, where the reliability of an empirical potential can be evaluated. The surface energies and the surface relaxations of the three low-index surfaces, (100), (110), and (111) are presented in Table VII. The experimental surface-energy data included in Table VII, $E_{poly}^{expt.}$, are for polycrystalline solids. All of these are extrapolated values, directly from high-temperature experimental data[24] or through some modeling approaches on temperature dependencies of surface energy.[25,26] As has been mentioned, the fitting to the experimental surface-energy data was simply done so that the calculated lowest surface energy [that of (110) surface] becomes close to the polycrystalline data. The order among the low-index surface energies, $E(110) < E(100) < E(111)$ is now in agreement with experimental information,[5,6] even though no action was made to fit the order. The relaxations in Table VII are for unreconstructed surfaces. The available experimental information or the first-principles calculation results for the relaxations are also presented for comparison.

TABLE VI. Calculated point-defect properties. Values listed are the relaxed vacancy-formation energy $E_v^f$ (eV) and the activation energy of vacancy diffusion $Q$ (eV) in comparison with corresponding experimental data, the formation energy of a self-interstitial $E_I$ (eV), and its structure. The experimental vacancy-formation energies and the experimental activation energies of diffusion are from Ref. 21 and Ref. 22, respectively, except for the activation energy of diffusion for Cr, which is from Ref. 23.

| | $E_v^f$ | | $Q$ | | Self-interstitial | |
|---|---|---|---|---|---|---|
| | MEAM | expt. | MEAM | expt. | $E_I$ | Structure |
| Fe | 1.75 | 1.79 | 2.28 | 2.5 | 4.23 | [110] dumbbell |
| Cr | 1.91 | 1.80 | 2.61 | 3.1 | 3.90 | [110] dumbbell |
| Mo | 3.09 | 3.10 | 4.22 | 4.5 | 5.97 | [110] dumbbell |
| W | 3.95 | 3.95 | 5.56 | 5.5 | 8.98 | [110] dumbbell |
| V | 2.09 | 2.10 | 2.47 | 3.2 | 2.49 | [110] dumbbell |
| Nb | 2.75 | 2.75 | 3.32 | 3.6 | 2.56 | [110] dumbbell |
| Ta | 2.95 | 2.95 | 3.71 | 4.3 | 4.88 | [110] dumbbell |

Finally, the properties calculated using the present 2NN MEAM potential are the thermal properties such as thermal-expansion coefficient, specific heat, melting, point, heat of melting and volume change on melting. The results are compared with available experimental data in Table VIII. Here, the melting points are those roughly estimated by heating, and therefore, should be regarded as an upper limit of the calculated melting points. The heat of melting is the value obtained at the calculated melting point of each element.

As can be seen in Tables IV–VIII, the present 2NN MEAM potentials reproduce the physical properties of the bcc transition metals fairly well, solving the problems that occured in the 1NN MEAM (Ref. 3) as mentioned in the Introduction. In the case of the properties where fitting was made, the agreement with experimental data is almost perfect. The calculations on the energy of simple cubic and diamond structures, on the self-interstitials, on the surface relaxations, and on the thermal properties are also reasonably good. The point that is not satisfactory is that the 2NN MEAM calculation according to the present parameters underestimates the energy of vacancy migration for most of the elements considered. Further, concerning V and Nb, the melting points are too low and atomic volumes of simple cubic and diamond structures are relatively too small. Generally, for V and Nb, the performance of the present 2NN MEAM seems to be worse than for the other elements.

Initially, it was intended to determine the potential parameters of the bcc elements keeping the values of $\beta^{(1)}$, $\beta^{(2)}$, and $\beta^{(3)}$ to be 1.0 as in the 1NN MEAM.[3] However, with these values, the calculated vacancy-migration energy and melting points for V and Nb were even worse than the present values. More decisively, it was found that the (100) surface of Nb undergoes a reconstruction into the *H*-induced-

TABLE VII. Calculated surface energies (erg/cm$^2$) and relaxations (%) of the low-index surfaces. $\Delta d_{ij}$ mean the change of interlayer spacing between the $i$th and $j$th layers, relative to corresponding bulk spacing. The experimental values are for polycrystalline solids and are those extrapolated from high-temperature experimental data to 0 K (Refs. 24 and 25) or to RT (Ref. 26). Values in the second or third row (if any) for each element are experimental or high-level calculation data for corresponding surface relaxation.

| | | (110) | | | (100) | | | (111) | | | | | |
|---|---|---|---|---|---|---|---|---|---|---|---|---|---|
| | $E_{poly}^{expt.}$ | $E_{(110)}$ | $\Delta d_{12}$ | $\Delta d_{23}$ | $E_{(100)}$ | $\Delta d_{12}$ | $\Delta d_{23}$ | $E_{(111)}$ | $\Delta d_{12}$ | $\Delta d_{23}$ | $\Delta d_{34}$ | $\Delta d_{45}$ | $\Delta d_{56}$ |
| Fe | 2360[a],2939[b] | 2356 | −1.5 | +0.1 | 2510 | −1.1 | +1.1 | 2668 | −10.5 | −16.5 | +12.2 | +0.5 | −6.0 |
| | | | 0[c] | | | −0.2[c] | +1.2[c] | | −16.9[c] | −9.8[c] | +4.2 [c] | −2.2[c] | |
| | | | | | | −1.5[d] | +0.0[d] | | | | | | |
| Cr | 2200[e],2056[b] | 2198 | −2.6 | +0.4 | 2300 | −0.8 | −0.7 | 2501 | −10.3 | −16.7 | +6.8 | +3.0 | −5.3 |
| Mo | 2900[e],2877[b] | 2885 | −3.3 | +0.6 | 3130 | −3.3 | +0.3 | 3373 | −14.0 | −16.4 | +5.5 | +3.5 | −4.3 |
| | | | −1.6[f] | | | −11[g] | +3[g] | | | | | | |
| W | 2990[a],3468[b] | 3427 | −3.0 | +0.4 | 3900 | −3.2 | −0.3 | 4341 | −13.2 | −17.0 | +7.2 | +2.4 | −4.0 |
| | | | −3.1[h] | +0.0 [h] | | −5.9[i] | | | −15.1[j] | −15.1[j] | +9.1[j] | | |
| | | | −3.0[k] | +0.2 [k] | | | | | | | | | |
| V | 2600[e],2876[b] | 2636 | −4.2 | +0.9 | 2778 | −7.3 | +3.8 | 2931 | −34.0 | −12.0 | +12.6 | −5.7 | −3.1 |
| | | | −0.3[l] | | | −6.7[l] | +1.0[l] | | | | | | |
| Nb | 2300[e],2983[b] | 2490 | −7.3 | +2.2 | 2715 | −12.5 | +3.0 | 2923 | −35.5 | −12.7 | +2.6 | +0.7 | −2.2 |
| Ta | 2780[e],3018[b] | 2778 | −3.5 | +0.6 | 3035 | −5.9 | +0.8 | 3247 | −19.2 | −17.2 | +12.4 | −0.6 | −4.9 |

[a]Reference 24.
[b]Reference 26.
[c]Reference 27.
[d]Reference 28.
[e]Reference 25.
[f]Reference 29.
[g]Reference 30 (calc.).
[h]Reference 31.
[i]Reference 32 (calc.).
[j]Reference 33 (calc.).
[k]Reference 34.
[l]Reference 35.

type structure[36] during an energy-minimization procedure, leaving the simply-relaxed $(1\times1)$ structure unstable. Even though it was known that the (100) surfaces of some bcc metals undergo a reconstruction,[37] it was believed that the simply-relaxed $(1\times1)$ structure should be at least metastable[38] against any reconstruction. In the present study, some efforts were made in order to make the (100) surface of Nb not to reconstruct directly from the ideal $(1\times1)$ structure, during energy minimization. It was found that such a reconstruction does not occur when a value greater than 2.0 is given to $\beta^{(2)}$, and the best overall results are obtained with a value of 2.5. Even though such a reconstruction did not occur on the (100) surface of V, it was found that improved results for the vacancy-migration energy and melting point could be obtained also by giving the same value 2.5 to $\beta^{(2)}$ of V. Therefore, the $\beta^{(2)}$ parameter of V was also given the new value. It was confirmed that such a change of $\beta^{(2)}$ value does not give a beneficial effect to the calculated properties of other elements considered.

It has been mentioned already that according to the present formalism the interactions between third nearest-neighbor atoms are not completely screened in the reference structure when the value of $C_{min}$ is low ($<0.47$ for bcc), while the pair potential is defined considering only the first and second nearest-neighbor interactions in all cases. This inconsistency causes an error in energy calculations even

TABLE VIII. Calculated thermal properties. Values listed are the thermal-expansion coefficient $\epsilon$ ($10^{-6}$/K), specific heat $C_p$ (J/mol K), melting point (K), heat of melting $\Delta H_m$ (KJ/mol) and volume change on melting $\Delta V_m/V_{solid}$ (%). The experimental data for thermal expansion coefficient, specific heat and volume change are from Ref. 22 and others are from Ref. 18.

| | $\epsilon$(0–100 °C) | | $C_p$(0–100 °C) | | Melting point | | $\Delta H_m$ | | $\Delta V_m/V_{solid}$ | |
|---|---|---|---|---|---|---|---|---|---|---|
| | MEAM | expt. | MEAM | expt. | MEAM | expt. | MEAM | expt. | MEAM | expt. |
| Fe | 12.4 | 12.1 | 26.1 | 25.5 | 2200 | 1811 | 13.2 | 13.8 | 3.4 | 3.5 |
| Cr | 9.0 | 6.5 | 26.8 | 24.0 | 2050 | 2180 | 18.8 | 21.0 | 4.4 | |
| Mo | 5.3 | 5.1 | 25.9 | 24.1 | 3100 | 2896 | 20.1 | 37.5 | 3.0 | |
| W | 4.2 | 4.5 | 25.4 | 25.4 | 4600 | 3695 | 33.0 | 52.3 | 3.2 | |
| V | 8.7 | 8.3 | 26.1 | 25.4 | 1800 | 2183 | 11.7 | 21.5 | 1.3 | |
| Nb | 6.4 | 7.2 | 26.1 | 24.9 | 1900 | 2750 | 13.5 | 30.0 | 1.0 | |
| Ta | 5.8 | 6.5 | 25.7 | 25.7 | 3200 | 3290 | 22.3 | 36.6 | 2.1 | |

though the amount is negligible. It has been also mentioned that a radial cutoff function with a cutoff distance between second and third nearest-neighbor distances was used in the present study in order to minimize the effect of such third nearest-neighbor interactions. Actually, all calculations presented in this section are those obtained using such radial cutoff distances for individual elements. These are 3.6 Å for Fe, Cr and V, 3.8 Å for Mo and W, and 4.0 Å for Nb and Ta. However, it is impossible to keep a value of the cutoff distance for each element, especially when dealing with an alloy system where each element has its own value of radial cutoff distance. Further, the calculations using empirical potentials are known to be significantly dependent on the selected value of radial cutoff distance.[39] Therefore, it is of practical importance to see how much the present 2NN MEAM formalism is dependent on the selected radial cutoff distances.

In empirical potentials, radial cutoff functions are used in order to confine the number of neighbors of an atom to a reasonable value, considering the stability of calculation results and computing time. Without any many-body screening, it is natural to obtain different results depending on the radial cutoff distance, that is, depending on the number of interacting neighbors of an atom. In the case of the present 2NN MEAM that uses the many-body screening, such a dependence on the radial cutoff distance is small compared to other empirical potentials, as long as the cutoff distance is larger than the second nearest-neighbor distance. Actually, such a dependence is absent when the $C_{min}$ is larger than 0.47, and is negligible even when the $C_{min}$ is smaller than 0.47 as already mentioned. However, this is not the only source of the dependency on the radial cutoff distance in empirical potentials. The existence of the radial cutoff itself can cause a dependence of 0 K calculations on the cutoff distance. This normally originates from relaxations, as explained below.

When the size of the radial cutoff distance is between second and third nearest-neighbor distances, the third nearest-neighbor interactions are not included in the calculation even when they exist due to no or incomplete many-body screening. However, in a structure with defects, relaxations can occur in a way to reduce some of the third nearest-neighbor distances near the defects. Such third nearest-neighbor interactions may be included in calculations depending on the size of radial cutoff distance. This means that there can be a dependence on the radial cutoff distance even when the cutoff distance is smaller than the third nearest-neighbor distance. On the other hand, with the present values of $C_{min}$ for individual elements, the second nearest-neighbor interactions and sometimes even third nearest-neighbor interactions are not completely screened in fcc, hcp, and other structures considered. Therefore, the energies of these structures also depend on the selected radial cutoff distance. The present radial cutoff distance for each element is smaller than the second nearest-neighbor distance of the fcc structure of corresponding element. The dependence on the radial cutoff distance is largest for the element with smallest $C_{min}$ value, but completely disappears if a radial cutoff distance larger than third nearest-neighbor distances of all structures considered is selected.

In the present study, the smaller values of the radial cutoff distances as described above were used for individual elements. This was to keep consistency with the pair potential defined considering only first and second nearest-neighbor interactions, and also to save computing time by decreasing the number of neighbor atoms for each atom. However, it is important to know how the results would differ for individual properties when a different radial cutoff distance, say the one larger than the third nearest-neighbor distance, is used. Radial cutoff distances larger than the third nearest-neighbor distances (4.5 Å for Fe, Cr, Mo, W, and V, and 5.0 Å for Nb and Ta) affect the calculated elastic constants of Fe, Nb, and Ta, the elements whose $C_{min}$ values are smaller than 0.47. The change of the $C_{11}$ of Ta was largest, and was from 2.664 to 2.649, which is not significant. The large radial cutoff distance also changes the calculated energies of all metastable structures, due to the inclusion of second and/or third nearest-neighbor interactions. The changes for Cr, Mo, W, and V are negligible, while those for Fe, Nb, and Ta are significant. For example, the energy difference between fcc and bcc, $\Delta E_{bcc\rightarrow fcc}$ changes from 0.069 to 0.048 eV, from 0.176 to 0.144 eV and from 0.148 to 0.104 eV, for Fe, Nb, and Ta, respectively. Even though the changes are not small, it is thought that the changes are still smaller than the error range of first-principles calculations. For Fe, the change is comparable to the error range of empirical thermodynamic assessments.[40] The effect of the large radial cutoff distances on the point-defect energies, the formation energy of a vacancy and of a self-interstitial, was relatively small. The vacancy-formation energy of Fe, Nb, and Ta was decreased by 0.05, 0.07, and 0.16 eV, respectively, by the use of large radial cutoff distances. The changes in the formation energy of a self-interstitial were smaller than those in the vacancy-formation energy. However, the changes in the activation energy of vacancy diffusion was significant. For Fe, Nb, and Ta, they were decreased by 10–15 %. This makes the agreement with experimental data even worse, because the calculated activation energies of vacancy diffusion are already smaller than the experiments for most of the elements considered, as shown in Table VI. The effect of radial cutoff distances on the surface relaxations was negligibly small. This is because the number of third nearest-neighbor interactions on surfaces is smaller than that in bulk. It was confirmed that the low-temperature thermal properties, $\epsilon$ and $C_p$ at 0–100 °C are not affected significantly by the radial cutoff distances. On the other hand, there seems to be some certain effect of the radial cutoff distances on the calculated melting points. For example, the calculated melting point of Fe changes from about 2200 K to 2060 K under the same heating rate when the large radial cutoff distance is used. However, these changes were not investigated in more detail because the calculated melting points listed in Table VIII were already quite approximate.

Now, it should be said that changing the radial cutoff distance gives certain effects on the calculated property values. However, in most cases, the changes due to using different cutoff distances are well within uncertainty ranges of

the experimentally measured or FP-calculated property values. Any radial cutoff distance greater than the second nearest-neighbor distance can be used without reducing the reliability of the present 2NN MEAM potential. The only exception is that the activation energies of diffusion that are lower than experimental values for most of the elements considered will become even lower if larger radial cutoff distances than those used in the present study are used. For example, if the larger radial cutoff distance is used, the calculated activation energy of Fe is decreased from 2.28 to 2.03 eV, which is lower than experimental value of 2.5 (by about 20%). The low activation energy of diffusion would give effect on the kinetics of phase transformations though it would not on the local equilibria. This should be kept in mind during practical applications of the present 2NN MEAM.

Finally, it should be noted that several different methods to include the second and more distant nearest-neighbor interactions were tested during this work; including second nearest-neighbor interactions without many-body screening, and including even third nearest-neighbor interactions without many-body screening were tested. However, using these methods, satisfactory results could not be obtained. For example, in the former case, the (110) surface energy, which should be the lowest became the highest among the three low-index surfaces, and in the latter case the energies of hcp structures became too high (several tenths of eV) compared to those of fcc structures. These problems could not be solved by simply changing the parameters. It was found that the correct order in the surface energies and overall agreements with experiments for all properties considered can be obtained only when the second nearest-neighbor interactions are partially included by adjusting the many-body screening, as has been done in the present study. The present 2NN MEAM formalism becomes exactly the same as the original 1NN MEAM if the second nearest-neighbor interactions are completely screened by adjusting the $C_{min}$ value. Letting each element have its own $C_{min}$ value, the two MEAM formalisms can easily be combined to describe alloy potentials among elements with various equilibrium structures, without changing the readily available parameters for elements with other structures.[3,4]

## V. SUMMARY

The second nearest-neighbor MEAM formalism has now been applied to all of the bcc transition metals. The potential parameters were determined systematically by fitting to $(\partial B/\partial P)$, elastic constants, structural energy differences among bcc, fcc and hcp structures, vacancy-formation energy, and surface energy. It was shown that the atomic potentials for the bcc transition metals according to the present 2NN MEAM reproduce structural properties of simple cubic and diamond structures, activation energy of diffusion, formation energy and structure of self-interstitials, surface relaxations, thermal-expansion coefficient, specific heat, melting point, and heat of melting satisfactorily, as well as the properties where fitting was made. It was also shown that though there exist certain effects of the size of radial cutoff distance on the calculation, they are not so severe as to decrease the applicability of the potential. The formalism is completely compatible with the original first nearest-neighbor MEAM that has been successfully applied to fcc, hcp, and other structured elements, does not give any additional difficulty in alloy descriptions, and, therefore, can be used to describe wide range of elements and alloy systems.

## ACKNOWLEDGMENTS

This work has been financially supported by the Korea Ministry of Science and Technology and the U.S. Department of Energy, Office of Basic Energy Sciences (MIB).

*FAX:+82-42-868-5032. Email address: bjlee@kriss.re.kr
†FAX: 505-667-8021. Email address: baskes@lanl.gov

[1] M.I. Baskes, Phys. Rev. Lett. **59**, 2666 (1987).
[2] M.I. Baskes, J.S. Nelson, and A.F. Wright, Phys. Rev. B **40**, 6085 (1989).
[3] M.I. Baskes, Phys. Rev. B **46**, 2727 (1992).
[4] M.I. Baskes and R.A. Johnson, Modell. Simul. Mater. Sci. Eng. **2**, 147 (1994).
[5] B.E. Sundquist, Acta Metall. **12**, 67 (1964).
[6] H.E. Grenga and R. Kumar, Surf. Sci. **61**, 283 (1976).
[7] M.I. Baskes, J.E. Angelo, and C.L. Bisson, Modell. Simul. Mater. Sci. Eng. **2**, 505 (1994).
[8] M.I. Baskes, Mater. Chem. Phys. **50**, 152 (1997).
[9] B.-J. Lee and M.I. Baskes, Phys. Rev. B **62**, 8564 (2000).
[10] M.I. Baskes, Mater. Sci. Eng., A **261**, 165 (1999).
[11] J.H. Rose, J.R. Smith, F. Guinea, and J. Ferrante, Phys. Rev. B **29**, 2963 (1984).
[12] P. Honenberg and W. Kohn, Phys. Rev. **136**, B864 (1964); W. Kohn and L.J. Sham, Phys. Rev. **140**, A1133 (1965).
[13] J.P. Perdew, in *Electronic Structure of Solids '91*, edited by P. Ziesche and H. Eschrig (Akademie Verlag, Berlin, 1991), p. 11; J.P. Perdew, J.A. Chevary, S.H. Vosko, K.A. Jackson, M.R. Pederson, D.J. Singh, and C. Fiolhais, Phys. Rev. B **46**, 6671 (1992).
[14] G. Kresse and J. Hafner, Phys. Rev. B **47**, R558 (1993); G. Kresse and J. Furthmüller, *ibid.* **54**, 11 169 (1996).
[15] D. Vanderbilt, Phys. Rev. B **41**, 7892 (1990); G. Kresse and J. Hafner, J. Phys.: Condens. Matter **6**, 8245 (1994).
[16] G. Simmons and H. Wang, *Single Crystal Elastic Constants and Calculated Aggregate Properties: A Handbook*, 2nd ed. (MIT Press, Cambridge, 1971).
[17] P. Bujard, Ph.D. thesis, University of Geneva, 1982.
[18] A.T. Dinsdale, CALPHAD: Comput. Coupling Phase Diagrams Thermochem. **15**, 317 (1991).
[19] A.T. Paxton, M. Methfessel, and H.M. Polatoglou, Phys. Rev. B **41**, 8127 (1990).
[20] F.W. Young, Jr., J. Nucl. Mater. **69/70**, 310 (1978).
[21] B. Zhang, Y. Ouyang, S. Liao, and Z. Jin, Physica B **262**, 218 (1999), and references therein.
[22] *Smithells Metals Reference Book*, 7th ed., edited by E.A. Brandes and G.B. Brook (Butterworth-Heinemann, Oxford, 1992).
[23] J. Askill and G.H. Tomlin, Philos. Mag. **11**, 467 (1965).

[24] W.R. Tyson and W.A. Miller, Surf. Sci. **62**, 267 (1977).
[25] M. I. Baskes and B. Hyland (private communication).
[26] L.Z. Mezey and J. Giber, Jpn. J. Appl. Phys., Part 1 **21**, 1569 (1982).
[27] J. Sokolov, F. Jona, and P.M. Marcus, Solid State Commun. **49**, 307 (1984); J. Sokolov, F. Jona and P.M. Marcus, Phys. Rev. B **33**, 1397 (1986); H. Li, Y.S. Li, J. Quinn, D. Tian, J. Sokolov, F. Jona, and P.M. Marcus, *ibid.* **42**, 9195 (1990).
[28] R. Imbihl, R.J. Behm, and G. Ertl, Surf. Sci. **123**, 129 (1982).
[29] L. Morales de la Garza and L.J. Clarke, J. Phys. C **14**, 5391 (1981).
[30] X.W. Wang, C.T. Chan, K.M. Ho, and W. Weber, Phys. Rev. Lett. **60**, 2066 (1988).
[31] M. Arnold, G. Hupfauer, P. Bayer, L. Hammer, K. Heinz, B. Kohler, and M. Scheffler, Surf. Sci. **382**, 288 (1997).
[32] C.T. Chan and S.G. Louie, Phys. Rev. B **33**, 2861 (1986).
[33] N.A.W. Holzwarth, J.A. Chervenak, C.J. Kimmer, Y. Zeng, W. Xu, and J. Adams, Phys. Rev. B **48**, 12 136 (1993).
[34] G. Teeter, J.L. Erskine, F. Shi, and M.A. Van Hove, Phys. Rev. B **60**, 1975 (1999).
[35] D.L. Adams, H.B. Nielsen, and J.N. Andersen, Phys. Scr., T **4**, 22 (1983).
[36] D. Singh and H. Krakauer, Phys. Rev. B **37**, 3999 (1988).
[37] M.K. Debe and D.A. King, Phys. Rev. Lett. **39**, 708 (1977).
[38] A.J. Melmed, S. T. Ceyer, and W. R. Graham, Surf. Sci. **111**, L701 (1981).
[39] H. Balamane, T. Halicioglu, and W.A. Tiller, Phys. Rev. B **46**, 2250 (1992).
[40] A. Fernández Guillermet and P. Gustafson, High Temp.-High Press. **16**, 591 (1985), and references therein.